Journal of Orthopaedic Translation (2019) 16, 102–111

Available online at www.sciencedirect.com

ScienceDirect

journal homepage: http://ees.elsevier.com/jot

ORIGINAL ARTICLE

Biomechanical evaluation of location and mode of failure in three screw fixations for a comminuted transforaminal sacral fracture model☆

Brett D. Crist [a,*], Ferris M. Pfeiffer [a,b], Michael S. Khazzam [c], Rebecca A. Kueny [d], Gregory J. Della Rocca [a], William L. Carson [b]

[a] *Department of Orthopaedic Surgery, University of Missouri, Columbia, 1100 Virginia Ave., Columbia, MO 65212, USA*
[b] *Thompson Laboratory for Regenerative Orthopaedics, University of Missouri, Columbia, 1100 Virginia Ave., Columbia, MO 65212, USA*
[c] *Department of Orthopaedic Surgery, University of Texas Southwestern Medical Center, Dallas, 1801 Inwood Road, Dallas, TX 75390, USA*
[d] *Institute of Biomechanics, TUHH Hamburg University of Technology, Denickestraße 15, 21073, Hamburg, Germany*

Received 21 March 2018; received in revised form 12 June 2018; accepted 20 June 2018
Available online 10 July 2018

KEYWORDS
bone–implant failure;
external fixator;
fracture stabilisation;
pelvic ring injury;
pelvic screws;
transforaminal sacral fracture

Abstract *Background:* Pelvic ring–comminuted transforaminal sacral fracture injuries are rotationally and vertically unstable and have a high rate of failure.
Objective: Our study purpose was to use three-dimensional (3D) optical tracking to detect onset location of bone–implant interface failure and measure the distances and angles between screws and line of applied force for correlation to strength of pelvic fracture fixation techniques.
Methods: 3D relative motion across sacral–rami fractures and screws relative to bone was measured with an optical tracking system. Synthetic pelves were used. Comminuted transforaminal sacral–rami fractures were modelled. Each pelvis was stabilised by either (1) two iliosacral screws in S1, (2) one transsacral screw in S1 and one iliosacral screw in S1 and (3) one trans-alar screw in S1 and one iliosacral screw in S1; groups 4–6 consisted of fixation groups with addition of anterior inferior iliac pelvic external fixator. Eighteen-instrumented pelvic

☆ This research was given as part of a podium presentation at the OTA's Annual Meeting, held in Baltimore, MD in October, 2010.

* Corresponding author. University of Missouri Department of Orthopaedic Surgery, One Hospital Dr., Columbia, MO 65212. USA.
E-mail addresses: cristb@health.missouri.edu (B.D. Crist), pfeifferf@health.missouri.edu (F.M. Pfeiffer), michael.khazzam@utsouthwestern.edu (M.S. Khazzam), becca.kueny@gmail.com (R.A. Kueny), dellaroccag@health.missouri.edu (G.J. Della Rocca), CarsonWL@msn.com (W.L. Carson).

https://doi.org/10.1016/j.jot.2018.06.005

models with right ilium fixed simulate single-leg stance. Load was applied to centre of S1 superior endplate. Five cycles of torque was initially applied, sequentially increased until permanent deformation occurred. Five cycles of axial load compression was next applied, sequentially increased until permanent deformation occurred, followed by axial loading to catastrophic failure. A Student t test was used to determine significance ($p < 0.05$).
Results: The model, protocol and 3D optical system have the ability to locate how subcatastrophic failures initiate. Our results indicate failure of all screw-based constructs is due to localised bone failure (screw pull-in push-out at the ipsilateral ilium—screw interface, not in sacrum); thus, no difference was observed when not supplemented with external fixation.
Conclusion: Inclusion of external fixation improved resistance only to torsional loading.
Translational Potential of this Article: Patients with comminuted transforaminal sacral—ipsilateral rami fractures benefit from this fixation.

Introduction

Comminuted transforaminal sacral fractures are components of unstable pelvic ring injuries and are associated with high-energy mechanisms like motor vehicle accidents. These sacral fractures are rotationally and vertically unstable [1] and have a relatively high rate of failure [2,3]. These injuries are often managed with various number of percutaneous iliosacral screws with or without anterior ring fixation. Clinically, predominant mode of failure is at bone—implant interface because of screw loosening and migration through sacrum-ilium, with few reported cases of screw bend or fatigue fracture [2,4—12]. Fixation failures are attributed to poor bone quality [8], infection [7,9—11], delayed and nonunions [9—11] and patient noncompliance [11,13]. Detecting onset location of bone—implant failure, effect of screw orientation distances and strength of construct will help guide fixation improvement. Knowledge of failure location, onset and effect of screw orientation and distances will allow clinicians to concentrate fixation improvement efforts at that location. Routt et al. [9—11] advocated the use of an additional screw to lock threads when an initial iliosacral screw obtains poor purchase but gave no scientific proof on how relative angle between screws improved fixation. Van Zwienen et al. [14] found no difference in construct strength with parallel versus converging screws, but angles between screws were not reported. Humphrey et al. [15] reported superior strength for constructs with two iliosacral screws locked to plate versus single screw construct.

Although previous biomechanical tests measured three-dimensional (3D) relative motion across pelvic fracture sites during increasing cyclic loading [16—21], we are unaware of any study that detected onset location of bone—implant failure or quantitatively measured and correlated strength of fixation to interscrew distances and angular orientations for trans—sacral—alar—iliac constructs. One previous study used optical tracking and sequential increasing cyclic load to examine pedicle screw migration and pull-out, with and without bioactive cement augmentation in osteoporotic bone [22]. Other biomechanical studies have examined stability of posterior pelvic ring fixation techniques [4,14—21,23—43]. Results are inconclusive because of uncontrolled dimensional and bone quality when using cadaveric specimens and testing protocol variabilities such as single versus bilateral stance, loading protocols modes of application and different parameter measures reported. In some cases, protocols did not mimic *in vivo* unconstrained motion between pelvic components.

Despite several biomechanical studies supporting the use of two iliosacral screw constructs for fixation of pelvic ring injuries, there remains debate as to its ability to provide adequate stabilisation of vertically unstable sacral fractures. Griffin et al. [2] found significant association of failure with vertical sacral fracture patterns compared to sacroiliac joint disruptions treated with iliosacral screws. Some clinicians have used longer screws (trans-alar and transsacral) to effectively increase area of fixation [2,4,44—47]. Also, additional fixation of fractured anterior rami significantly reduces its gapping [48].

Our purpose was to investigate if 3D optical tracking can detect onset and location of bone—implant interface failure and if it can measure distances and angles between screws and the line of applied force for correlation to strength of commonly used pelvic ring fracture fixation strategies.

Methods

By attaching a light-emitting diode (LED) block to each, the 3D motion of pelvic components and screws relative to one another was measured using an NDI Certus Optotrak (Northern Digital, International, Waterloo, Ontario, Canada) tracking system (±0.01 mm resolution). The LED blocks were attached to hex rods inserted into the hex of screw heads. Figure 1 illustrates general direction of axes and + directions of motion. 3D components of relative motion (Δx,Δy,Δz,Rx,Ry,Rz) of a point in and rotation of (assumed rigid) bodies measured and evaluated were as follows:

1) Centre of S1 endplate relative to right ipsilateral ilium (+z cranial and parallel to pushrod initially).

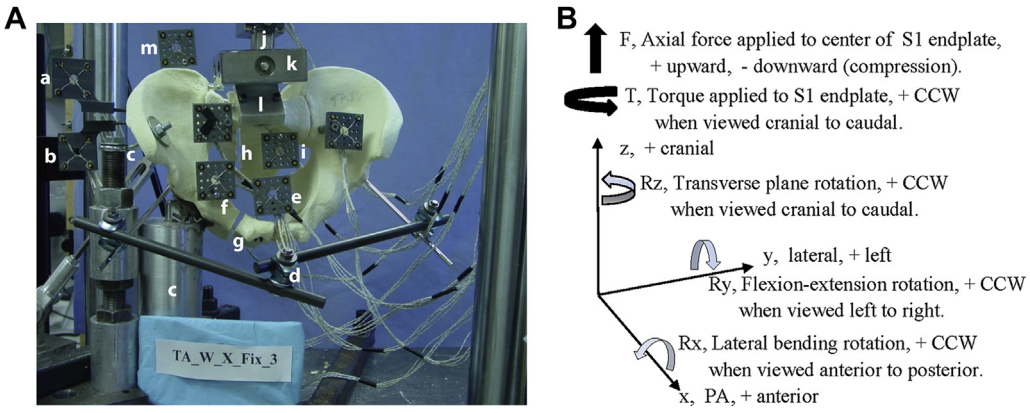

Figure 1 A). Pelvic specimen mounted in an Instron biaxial test cell, with LED blocks in place. a, screw 2 LED block; b, screw 1 LED block; c, single-leg stance supports for the right ilium; d, anterior inferior iliac pelvic external fixator; rami LED blocks at e, the contralateral segment, and f, the ipsilateral segment; comminuted fracture at g, rami, and h, transforaminal sacral; i, sacrum LED block; j, pushrod; k, U-joint and attachment; l, S1 endplate; and m, right ilium LED block. (B). Definitions axes, directions of motion and applied loads. Applied loads: force and torque were applied to the centre of the S1 endplate, via a pushrod with universal joint and attachment—positive force upward, negative force downward (compression) and positive torque CCW when viewed cranial to caudal. Global axes: Rz is transverse plane rotation, with positive direction CCW when viewed cranial to caudal. Ry is flexion-extension rotation, with positive direction CCW when viewed left to right. Rx is lateral bending rotation, with positive direction CCW when viewed anterior to posterior. Screw axes: Positive z direction is cranial, positive y is towards screw tip, and positive x is posterior. CCW = counterclockwise; LED = light-emitting diode.

2) Screw 1 (sacral, transsacral, trans-alar): point on its axis at head relative to ipsilateral ilium, point on its axis 80 mm from screw head relative to sacrum (+y axis coincident with screw axis pointing from head to tip, +z cranial and parallel to pushrod initially).
3) Screw 2 (sacral): Same as screw 1.
4) Centre of anterior contralateral segment of rami fracture relative to ipsilateral ilium's segment (+y to left and perpendicular to plane of 3 points digitised on perimeter of rami anterior fracture surface of contralateral segment, +z cranial and parallel to pushrod initially).

A synthetic pelvis model (foam; Sawbones Model 130-1, Pacific Research Laboratories, Vashon, WA) was used to eliminate variability in size, geometry and bone properties in cadaveric pelves [27]. Comminuted transforaminal sacral and rami fractures were simulated in a gap model [1] by sawing and removing a 0.5 cm section from the right sacrum, foramina, superior and inferior rami of each model. The section was replaced with removable 0.5 cm shim to prevent loss of gap during screw insertion. All native model hardware was removed prior to screw-fixator placement. Eighteen pelvic models were randomly assigned and instrumented creating six different fixation groups (n = 3 per group): (1) two iliosacral screws in S1 (SI group); (2) one iliosacral, one transsacral screw in S1 (TS group) and (3) one iliosacral, one trans-alar screw in S1 (TA group); groups 4–6 included addition of an anterior inferior pelvic external fixator (DePuy Synthes Large External Fixator, West Chester, PA) to constructs in groups 1–3. Partially-threaded (16 mm) 6.5 mm outer diameter cannulated screws were used, with the following lengths: iliosacral, 85 mm; trans-alar, 125 mm; and transsacral, 160 mm (DePuy Synthes, USA).

Iliosacral screws were inserted using standard percutaneous operative technique [44,45]. Each screw (washer on inferior screw only) was placed over a guide wire through posterior ilium and into vertebral body of S1 (iliosacral), to opposite sacral ala (trans-alar), or into opposite ilium (transsacral). An anterior external fixator was used in half of the constructs. Each model was tested in a physiological single right-leg stance, right acetabulum supported with a hemiarthroplasty implant that allowed unconstrained relative rotation between the ball-and-socket. Iliac crest was restrained from rotation by two custom-made supports to simulate the hip abductor muscle group (Figure 1).

Axial force and transverse plane torque were applied to the superior endplate of S1 by a 112 cm pushrod with universal joints on each end. This ensured only axial load and transverse torque were applied, both acting along and about an axis remaining nearly vertical, in mid-sagittal plane and through the centre of the superior S1 endplate. Thus, 3D motion of S1 relative to right ilium was unconstrained, with exception of axial translation—rotation. An Instron 8821S biaxial testing machine (Norwood, MA, USA) with a 25 kN ± 250Nm load cell attached to ram was used in position control. Ram was rotated using a constant velocity (±0.2°/second) ramp function to apply cyclic reverse direction torque while holding the test machine's ram at initial "no load" axial position. To apply a cyclic axial compressive load, a constant velocity (0.1 mm/s) ramp function was used while holding the ram's rotation at initial "no load" position. A limit detect stopped each ramp at desired maximum and minimum load levels. Five cycles of ±10Nm torque were initially applied and then sequentially increased by 5Nm until permanent deformation occurred (detected by offset of 5° ram rotation at zero torque at end of a cycle). Five cycles of 15N–50N axial compression were applied, then maximum compression sequentially increased

by 50N until permanent deformation occurred (detected by 2 mm offset in ram axial position when cycle returned to 15N compression). This was followed by axial loading to catastrophic failure, except one trans-alar with fixator and one trans-alar without fixator construct that were loaded counterclockwise (CCW, +T) to determine torsion to failure.

Applied force (F) and torque (T), ram axial and rotary position and 3D spatial position of LEDs in blocks were digitally recorded at 10Hz as load was applied. NDI Optotrak software (Northern Digital, International, Waterloo, Ontario, Canada) was used to determine the aforementioned components of relative motion. Flexibility coefficients of a specimen were determined by finding inverse slope of linear portion of first cycle of applied load ($-10 < F < -50$N for axial load) and ($-4<T- < -1$ and $1 < T+<4$Nm for torsional load) versus each component of displacement (Δx,Δy,Δz,Rx,Ry,Rz) of sacrum relative to ilium.

The motion of screw 1 (point on head) and screw 2 (point 80 mm from head) relative to the ipsilateral ilium and sacrum were of particular interest in this study to determine the onset and location (ilium or sacrum) of screw–bone interface failure. To do a quantitative comparison of the load resistance capabilities of SI, TS, TA screw combinations with and without the external fixator, the displacement components at the maximum load of the fifth cycle of each applied load ($F = -50$, -100, -150, -200 and -250N and $T = \pm 10$, ± 15 and ± 20Nm) were extracted and plotted as a function of the corresponding applied load. A similar plot was generated for the first load cycle. For a statistical comparison, components of displacement at the fifth cycle of the maximum axial load reached by all constructs ($F = -150$N) were determined. Reverse direction torsional load range of motion (ROM) was determined by subtracting the displacement at $T = -15$Nm from displacement at $T = +15$.

The optical tracking's LED position data were used to calculate before loading commenced: distance between screw heads, common perpendicular distance between screws and corresponding angle between them and perpendicular distance of screw 1 and 2 from line of action of applied force F to determine if they correlate to failure modes. Flexibility coefficients (of S1 relative to the ipsilateral ilium) associated with the anticipated major components of motion was plotted as function of the aforementioned screw parameters to determine if a correlation existed. Applied load as function of ram displacement was plotted to determine the load at onset of failure (first sharp drop in load) and at ultimate failure (maximum load resisted). Video was taken of each test to confirm externally visible modes of failure and relative motion of the pelvic ring components. Student *t* test (two tail, unequal variance) was used to determine significance ($p < 0.05$).

Results

General

Figure 2 shows the 3D components of relative displacement (Δx,Δy,Δz) and rotation (Rx,Ry,Rz) for each of the four rigid bodies mentioned above plotted as a function of applied load for the entire test. This provides an overall view of the relative motion's magnitude and direction, and it determines if irreversible motion (motion increasing with each cycle at same load level) occurs. Irreversible motion is

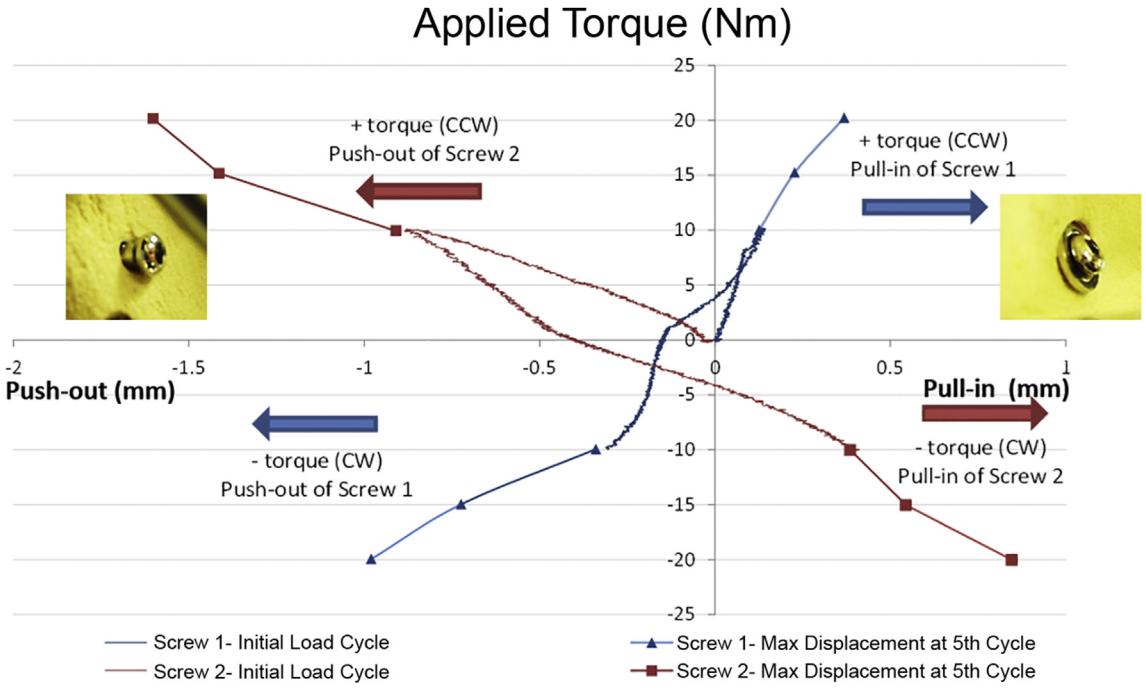

Figure 2 Example of screw 1 and 2's Δy (push-out, pull-in) component of motion relative to ipsilateral ilium during torsional cyclic loading. CCW = counterclockwise.

indicative of material yield-crush at a screw—bone interface. Figure 3A contains an example illustrating axial loading and significant irreversible progression of increasing displacement/cycle of screw rotation about its axis Ry relative to the ipsilateral ilium. It also shows a slight irreversible progression of the lateral bending rotation Rx, a nearly reversible transverse plane rotation and no signs of irreversible motion relative to the sacrum. In Figure 3B, significant progression primarily occurred as screw rotation Ry about its axis relative to the ilium, with resulting progression of related motion components between sacrum, ipsilateral ilium and rami.

Effect of external fixation

Without anterior external fixation (WOX), there were no statistical differences between the SI, TS, TA constructs in flexibility (Table 1), motion across rami fracture (Table 2), motion of sacrum relative to ipsilateral ilium (Table 3) and initial and maximum failure force F (Table 4). With anterior fixation (WX), there were also no significant differences between constructs in flexibility, ultimate strength or rami motion.

Torsional loading—effect of external fixation

WX versus WOX consistently produced differences in average values of potentially clinical significance in SI, TS and TA constructs. It reduced sacrum flexibility transverse plane rotation Rz (Table 1), and it reduced rami fracture opening—closing Δy (Table 2) as well as transverse plane rotation Rz (Table 2). Fixation (WX) produced some differences in rami fracture motion (Table 2). WX produced consistent changes in sacral motion relative to ipsilateral ilium (Table 3); there was reduction in AP translation Δx and transverse plane rotation Rz, and there was a change in direction of lateral bend rotation Rx.

Axial loading—effect of external fixation

For axial loading, WX versus WOX produced no differences between the three constructs except for reduced sacrum flexibility to flexion rotation in one case (Table 1), rami fracture flexion rotation in two cases (Table 2) and sacrum relative to ipsilateral ilium rotation in two cases (Table 2). WX produced no statistical difference in initial failure force F or maximum failure force (one exception Table 4). Catastrophic failure occurred as fracture of ipsilateral ilium, typically through screw—bone interface.

Screw motion relative to ipsilateral ilium

Predominant average ROM components of screws were at the fifth cycle of −150N compressive force F: flexion rotation Ry about their axis (Screw 1, 2) and lateral bend rotation Rx (Screw 1,2). Transverse plane ROM Rz of screws for WX and WOX was relatively small. General 3D rotation of sacrum relative to ipsilateral ilium visually appeared as pivoting in vicinity of the screw—ilium interfaces for WX and WOX, an observation consistent with a relatively small translation of screw heads.

The highest average ROM components of screws for torsional loading were flexion rotation Ry about their axis and transverse plane rotation Rz. General 3D rotation of

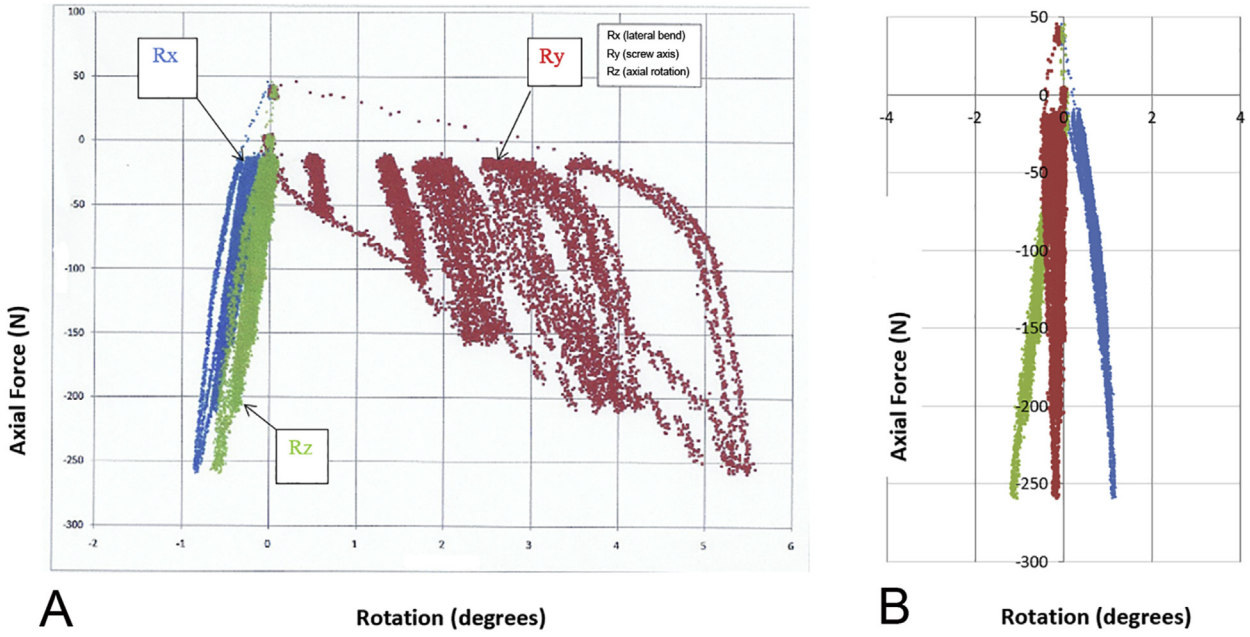

Figure 3 Screw 1 components of rotation (Rx lateral bend, Ry about screw axis, Rz transverse plane) during five cycles of axial compressive loading: from −10 to −50 N, then to −100, −150, −200, −250. (A) Screw rotation relative to the ipsilateral ilium. Rx—slight irreversible progression of increasing displacement per cycle. Ry—significant irreversible progression of increasing displacement per cycle. Rz—very little displacement per cycle. (B) Screw rotation relative to the sacrum. No signs of increasing displacement per cycle relative to the sacrum of any of the components of motion.

Table 1 Flexibility of sacrum relative to ipsilateral ilium.

Flexibility coefficient		To torsional loading (1−4 Nm Rz+) (−1 to −4 Nm Rz-)			
		WX (with external fixator)		WOX (without external fixator)	
		Rz+ (deg/Nm)	Rz− (deg/Nm)	Rz+ (deg/Nm)	Rz− (deg/Nm)
Construct	SI	0.26 ± 0.07[a]	0.25 ± 0.06	0.42 ± 0.13[a]	0.44 ± 0.10
	TS	0.20 ± 0.03[b]	0.24 ± 0.04	0.38 ± 0.01[a,b]	0.44 ± 0.05
	TA	0.21 ± 0.04[c]	0.26 ± 0.04	0.34 ± 0.01[a,b,c]	0.36 ± 0.03
	All	0.22 ± 0.05[d]	0.25 ± 0.04[e]	0.38 ± 0.07[d]	0.41 ± 0.07[e]

To axial compression loading (−10 to −50 N)							
Flexibility coefficient		z (mm/KN)	Rx (deg/KN)	Ry (deg/KN)	z (mm/KN)	Rx (deg/KN)	Ry (deg/KN)
Construct	SI	5.8 ± 1.5	4.6 ± 0.6	−7.6 ± 1.0 f	18.1 ± 9.1	6.3 ± 1.5	−39.1 ± 29.0
	TS	9.4 ± 3.4	5.5 ± 2.7	−11.7 ± 5.3	13.4 ± 4.4	7.4 ± 2.1	−15.9 ± 1.0[f]
	TA	18.7 ± 9.3	4.8 ± 1.1	−31.0 ± 17.6	10.3 ± 3.1	6.2 ± 3.0	−14.6 ± 4.4
	All	11.3 ± 7.6	5.0 ± 1.6	−16.7 ± 14.2	13.9 ± 6.3	6.6 ± 2.1	−23.2 ± 18.9

WOX = without anterior external fixation; WX = with anterior fixation.
[a, b, c]WOX is significantly more flexible than WX, pooled Rz+ with Rz- data ($p < 0.0075$, n = 6)
[d, e]WOX is significantly more flexible than WX, pooled SI, TS, TA ($p < 0.00014$, n = 9)
z: Only TS WOX approached being more flexible than SI WX ($p = 0.08$), all others $p > 0.13$
Rx: WOX flexibility was not different than WX of same or other constructs, $p > 0.13$,
Approaching significance ($p = 0.07$) for pooled SI, TS, TA.
f Ry: Only TS WOX was more flexible than SI WX ($p = 0.006$), all others $p > 0.1$

Table 2 Rami motion: contralateral segment of ipsilateral rami relative to ipsilateral rami.

Displacement at 5th cycle of max compression to 150 N							
Construct:		x (mm) AP shear	y (mm) Open/close	z (mm) CrCa shear	Rx (deg) Lat. bend	Ry (deg) Flex/Ext	Rz (deg) Tran Plane
WX	SI	−2.5 ± 0.6	−0.7 ± 0.7	−2.7 ± 0.5	−1.0 ± 0.1	1.0 ± 0.3[b]	1.0 ± 0.2
	TS	−2.3 ± 1.6	−0.4 ± 0.8	−3.0 ± 1.2	−0.6 ± 0.5	0.9 ± 0.8	0.7 ± 0.2
	TA	−5.7 ± 1.9[a]	−0.3 ± 1.4	−4.0 ± 0.9	−0.6 ± 1.3	2.5 ± 0.6[b,c,d]	1.4 ± 0.5
WOX	SI	0.3 ± 8.3	0.6 ± 1.1	−7.1 ± 5.0	−1.3 ± 0.5	3.1 ± 1.5	0.9 ± 0.8
	TS	−2.6 ± 2.0	−0.1 ± 1.0	−3.4 ± 0.4	−0.8 ± 1.0	1.1 ± 0.4[d]	1.0 ± 0.8
	TA	−1.5 ± 0.7[a]	0.2 ± 0.9	−2.8 ± 0.5	−0.8 ± 0.7	0.9 ± 0.5[c]	0.8 ± 0.4

Range of motion (ROM) during 5th cycle of torsional loading from −15 to +15 Nm							
Construct:	x (mm)	y (mm)	z (mm)	Rx (deg)	Ry (deg)	Rz (deg)	
WX	SI	1.4 ± 4.0	−0.8 ± 1.6[c]	3.2 ± 0.7[f]	−1.7 ± 1.9	−5.7 ± 3.2	4.6 ± 1.1[j]
	TS	1.1 ± 3.3	−0.6 ± 1.6[d]	2.2 ± 1.2[g]	−1.8 ± 0.2[g]	−5.2 ± 2.6	4.2 ± 1.0[k]
	TA	3.0 ± 1.4[a,b]	−0.4 ± 0.6[e]	3.0 ± 2.4	−1.7 ± 0.9[f]	−6.2 ± 1.0	5.0 ± 1.9[l]
WOX	SI	−5.6 ± 4.7	9.1 ± 0.5[c,d,e]	2.7 ± 5.4	−4.4 ± 6.1	−6.8 ± 7.8	6.0 ± 7.0
	TS	−3.8 ± 1.3[b]	11.2 ± 0.7[c,d,e]	6.8 ± 0.4[f,g]	1.5 ± 2.5	−8.0 ± 2.0	13.2 ± 3.1[j,k,l]
	TA	−1.2 ± 0.9[a]	9.3 ± 1.6[c,d,e]	5.8 ± 2.3	0.3 ± 0.8[f,g]	−7.3 ± 2.5	10.6 ± 0.6[j,k,l]

WOX = without anterior external fixation; WX, with anterior fixation.
x: [a]TA WX greater magnitude than TA WOX ($p = 0.046$), all others $p > 0.076$.
y: No significant difference between any constructs ($p > 0.25$)
z: No significant difference between any constructs ($p > 0.12$)
Rx: No significant difference between any constructs ($p > 0.18$)
Ry: [b,c,d]TA WX greater magnitude than other three ($p < 0.036$), all others $p > 0.064$.
Rz: No significant difference between any constructs ($p > 0.13$.)
x: [a,b]($p < 0.017$), all others $p > 0.06$.
y: [c,d,e]All WX less opening−closing than WOX ($p < 0.006$)
z: [f,g]($p < 0.014$), all other $p > 0.19$.
Rx: [h,i]($p < 0.040$), all other $p > 0.15$.
Ry: No significant difference between any constructs ($p > 0.36$)
Rz: [j,k,l]($p < 0.030$), all other $p > 0.21$.

Table 3 Sacrum motion: sacrum relative to ipsilateral ilium.

Displacement at 5th cycle of max compression to 150 N							
Construct:		x (mm) PA	y (mm) Lateral left	z (mm) CaCr	Rx (deg) Lat. bend	Ry (deg) Flex/Ext	Rz (deg) Tran Plane
WX	SI	0.48 ± 0.05	0.11 ± 0.11	−1.06 ± 0.19[a]	−0.71 ± 0.15	1.36 ± 0.17[c,d]	−0.22 ± 0.37
	TS	0.53 ± 0.23	0.08 ± 0.14	−1.36 ± 0.41	−0.68 ± 0.27	1.79 ± 0.65[e]	−0.13 ± 0.26
	TA	1.20 ± 0.71	0.09 ± 0.16	−2.31 ± 0.49[a]	−0.46 ± 0.21	3.70 ± 0.95[c,e,f]	−0.05 ± 0.17
WOX	SI	1.26 ± 0.96	−0.11 ± 0.48	−2.11 ± 0.89	−0.57 ± 0.30	4.29 ± 2.51	−0.57 ± 1.07
	TS	0.51 ± 0.17	0.18 ± 0.14	−1.93 ± 0.62	−0.98 ± 0.42	2.23 ± 0.34[d]	−0.09 ± 0.35
	TA	0.73 ± 0.30	0.32 ± 0.48	−1.67 ± 0.74	−1.00 ± 0.75	1.68 ± 0.48[f]	−0.22 ± 0.11
Range of motion (ROM) during 5th cycle of torsional loading from −15 to +15 Nm							
Construct:		x (mm)	y (mm)	z (mm)	Rx (deg)	Ry (deg)	Rz (deg)
WX	SI	−5.7 ± 1.8	2.7 ± 0.7[b]	1.1 ± 0.6	−0.4 ± 0.3[c]	−3.4 ± 1.9	7.8 ± 1.6
	TS	−4.5 ± 0.4[a]	3.2 ± 0.5	0.9 ± 0.3	−1.0 ± 0.9	−3.3 ± 1.6	7.3 ± 0.6[e]
	TA	−5.2 ± 0.3	4.4 ± 0.8[b]	1.6 ± 0.5	−1.2 ± 0.5[d]	−4.2 ± 0.2	8.3 ± 1.0
WOX	SI	−7.6 ± 3.1	4.2 ± 1.3	1.5 ± 1.6	0.9 ± 0.1[c,d]	−2.4 ± 4.0	12.6 ± 2.8
	TS	−10.8 ± 3.7	5.9 ± 2.4	1.0 ± 0.2	0.4 ± 1.3	−2.2 ± 2.5	15.2 ± 3.5
	TA	−6.5 ± 0.7[a]	3.8 ± 0.5	1.8 ± 0.6	1.1 ± 0.2[c,d]	−2.5 ± 1.4	10.8 ± 1.5[e]

WOX = without anterior external fixation; WX, with anterior fixation.
x: No significant difference between any constructs ($p > 0.22$)
y: No significant difference between any constructs ($p > 0.33$)
z: [a]($p < 0.034$), all others $p > 0.06$
Rx: No significant difference between any constructs ($p > 0.15$)
Ry: [c,d,e,f]($p < 0.052$), all others $p > 0.10$.
Rz: No significant difference between any constructs ($p > 0.22$)
x: [a]($p < 0.018$), all others $p > 0.06$.
y: [b]($p = 0.055$), all others $p > 0.10$.
z: No significant difference between any constructs ($p > 0.11$)
Rx: [c,d]($p < 0.011$), all others $p > 0.08$.
Ry: No significant difference between any constructs ($p > 0.17$)
Rz: [e]WX had lower ROM than any WOX, at or approach significance ($0.043 < p < 0.10$)

Table 4 Axial force F at failure.

Construct	Initial failure force F (N)		Maximum failure force F (N)	
	WX	WOX	WX	WOX
SI $_{n=3}$	−393 ± 69	−249 ± 141	−827 ± 34[a]	−438 ± 207
TS $_{n=3}$	−486 ± 171	−513 ± 157	−718 ± 74	−664 ± 54[a]
TA $_{n=2}$	−416 ± 226	−425 ± 43	−528 ± 269	−689 ± 59

WOX = without anterior external fixation; WX, with anterior fixation.
Initial: $p > 0.10$
Max: [a]($p = 0.017$), all others $p > 0.080$

screw–sacrum combination was transverse plane rotation that produced pull-in (+Δy) of screw 1 and push-out (-Δy) of screw 2 during positive torque (CCW), with opposite effect during negative torque [clockwise (CW); Figure 3].

Screw motion relative to sacrum

Rz motion appeared as reversible (not increasing each cycle of same applied torque) up through ±20Nm torque level. Reversible Rz motion along with small Rx motion implies screws were not wallowing out a cavity in sacrum by yield of screw–bone interface.

Large standard deviations occurred for all axial flexibility coefficients Δz,Rx,Ry. To investigate cause, geometric parameters were determined for screw 1 relative to 2: distance between screw heads, angle between screw axes, common perpendicular distance between screw axes and perpendicular distance to the line of applied axial force. No correlation existed between any coefficients or parameters.

Discussion

The purpose of this study was to determine if optical tracking could detect onset and location of failure initiation

and the potential to correlate distances and angles between screws and the line of applied force to strength of commonly used sacral fracture fixation techniques. A single-leg stance with unconstrained motion and a cyclic loading protocol using 3D optical tracking was developed. This model simulated normal physiological "worst case" internal loading and pelvic conditions and thus clinical failure. Compressive axial load simulated torso plus contralateral leg weight-bearing during single-leg stance. Reverse direction torsional loading simulated leg—body swing during walking and bed rolling. Since axial-torsional loading are primary external pelvic loading during early recovery, single-leg stance with addition of lateral or flexion-extension bending moment was not tested. Since axial load was anterior to screws, a flexion-bending moment existed at the ipsilateral ilium—screw interface, explaining why flexion rotations of screws about their axis of the sacrum and across the rami were observed. Thus, these results reveal relative resistance of the constructs to a flexion-bending moment.

Our axial and torsional loading tests showed no significant differences in load resistance or fracture stabilisation between SI, TS and TA constructs without anterior external fixation, and likewise, discounting a few comparisons, no differences between constructs with fixation were observed. Without anterior fixation, screw pairs acted similar to a cantilever beam, base support being ipsilateral ilium screw interface, with the sacrum transferring applied load to the opposite end of the beam. Load resistance capabilities of a cantilever are primarily dependent on strength characteristics of the base support, the location of the highest bending moment. Ipsilateral ilium—screw interface base supports were identical for all three constructs, explaining no differences between the SI, TS, TA and WOX constructs. Anterior external fixation provides additional support to the sacral end of cantilever beam, partly counteracting applied load on the sacrum. Anterior fixation does not alter ipsilateral ilium—screw base support, and this is consistent with the lack of differences between SI, TS and TA constructs with fixation. Forces transmitted to the sacral end of the cantilever by an anterior external fixator do alter some components of force and moment (bending moment about z axis) that occur at critical ipsilateral ilium—screw base support. This explains the significant reduction in the rami fracture opening—closing, the transverse plane rotation and the torsional flexibility of the sacrum relative to ipsilateral ilium for WX versus WOX. The reason for no differences between the SI, TS and TA constructs with use of a Sawbones pelvic model is that onset of bone—implant failure occurred at ipsilateral ilium, not within the sacrum.

The 3D components of screw motion in the sacrum were relatively small for axial—torsional loading, with exception of reversible transverse plane rotation Rz for torsional loading. Relatively high Rz rotation without sacral bone—screw interface deterioration implies nonrigid sacrum—screw bending was producing Rz measured motion. Our motion analysis was based on the assumption of the bodies being rigid. Reversible material deflection does not affect ability to detect onset and location of irreversible bone—implant interface deterioration or hardware bending-fracture.

These results are consistent with previous studies that have shown no differences between posterior fixation constructs. Van Zwienen et al. [20] reported two iliosacral screws in S1 versus a screw in S1, S2 were equivalent in preventing rotation and load failure. Simonian et al. [24] and Gorczyca et al. [26] compared methods of posterior fixation and reported no differences. Comstock et al. [25] showed two iliosacral screws restored about 80% of torsional and axial load of intact pelvis in a simulated cadaveric sacroiliac dislocation.

Two studies have shown differences between constructs that used posterior ring fixation. Yinger et al. [27] evaluated nine posterior-only fixation methods in synthetic pelvic models, simulating an SI joint dislocation and pubic symphyseal disruption. Constructs with two sacroiliac plates, two iliosacral screws or two sacroiliac plates with one iliosacral screw provided the highest resistance to sacroiliac joint gapping. In a transforaminal sacral fracture cadaveric model, Humphrey et al. [15] showed a locking plate construct led to significantly less fracture displacement after 10,000 cycles of subfailure axial loading, compared to fixation with one 7.3 mm cannulated screw. Neither studies compared either a trans-alar or transsacral screw to iliosacral screw constructs.

Anterior and posterior pelvic ring fixation is recommended for vertically unstable fracture patterns by Van den Bosch et al. [49]. Sagi et al. [23] evaluated a vertically unstable, sacroiliac dislocation model using fresh-frozen cadaveric pelvi and three different posterior fixation constructs. There was no difference in rotational or linear displacement between constructs that used one or two iliosacral screws, but adding anterior ring fixation (a pubic symphyseal plate) led to significantly less axial displacement of the SI joint and restored the same response to axial loading that was seen in the uninjured hemipelvis. Our results also emphasise the need for anterior ring fixation to minimise the risk of clinical failure.

The optical tracking system captured the relative 3D motion of multiple points on and body rotations between the ilium, sacrum, fracture surfaces and individual screws. This allowed us to determine resistance to loading and to potentially determine where and how sub-catastrophic failure is occurring. This study provides specific screw motion data and related insights into where and how sub-catastrophic failures initiate.

There are two primary limitations to our study. First, since the onset of bone—implant failure occurred in the ilium, we could not test our hypothesis that the longer screw constructs would be superior; to do so would require a pelvic model where failure occurs first in the sacrum (i.e., a model simulating osteoporotic sacral bone). Second, we did not use a protocol that could systematically control for a range of values in parameters such as distance between screw heads, angle between screw axes, common perpendicular distance between screw axes and perpendicular distance to the line of applied (anterior) axial force, for either screw axis. This may be the reason that we found no correlation between any of the axial and torsional load flexibilities and any of these.

Conclusions

The model, protocol and 3D tracking methods used here give insight into the location and nature of how sub-

catastrophic failures initiate. Failure of all three screw-based constructs was due to localised bone failure and screw pull-in and push-out at the ipsilateral ilium—screw interface and not in the sacrum. Thus, there was no difference in resistance to axial or torsional load when constructs were not supplemented with anterior pelvic external fixation. External fixation improved resistance only to torsional loading, thus patients with comminuted transforaminal sacral—rami fractures benefit from posterior—anterior pelvic ring fixation.

Funding

This project was made possible through the Orthopaedic Trauma Association's Basic Science Research Grant program.

Conflict of interest statement

Authors Brett D. Crist and Gregory J. Della Rocca are board or committee members of the Orthopaedic Trauma Association, and both receive unrelated research support from DePuy Synthes.

Acknowledgements

The authors thank DePuy Synthes (West Chester, PA, USA) for supplying the bone models and implants used for this project.

Appendix A. Supplementary data

Supplementary data related to this article can be found at https://doi.org/10.1016/j.jot.2018.06.005.

References

[1] Tile M. Acute pelvic fractures: I. Causation and classification. J Am Acad Orthop Surg 1996;4(3):143—51.
[2] Griffin DR, Starr AJ, Reinert CM, Jones AL, Whitlock S. Vertically unstable pelvic fractures fixtures with percutaneous iliosacral screws: does posterior injury pattern predict fixation failure? J Orthop Trauma 2006;20(1 Suppl):S30—6.
[3] Tile M. Pelvic ring fractures: should they be fixed? J Bone Joint Surg Br 1988;70(1):1—12.
[4] Beaulé PE, Antoniades J, Matta JM. Trans-sacral fixation for failed posterior fixation of the pelvic ring. Arch Orthop Trauma Surg 2006;126(1):49—52.
[5] Cole JD, Blum DA, Ansel LJ. Outcome after fixation of unstable posterior pelvic ring injuries. Clin Orthop Relat Res 1996;329:160—79.
[6] Gardner MJ, Routt Jr ML. Transiliac-transsacral screws for durable posterior pelvic stabilization. J Orthop Trauma 2011;25(6):378—84.
[7] Lindahl J, Hirvensalo E, Bostman O, Santavirta S. Failure of reduction with an external fixator in the management of pelvic ring injuries — long-term evaluation of 110 patients. J Bone Joint Surg 1999;81(6):955—62.
[8] Moed BR, Geer BL. S2 iliosacral screw fixation for disruptions of the posterior pelvic ring: a report of 49 cases. J Orthop Trauma 2006;20(6):378—83.
[9] Routt ML, Simonian PT, Inaba J. Iliosacral screw complications. Operative Techniques Orthop 1997;7(3):206—20.
[10] Routt ML, Simonian PT, Mills WJ. Iliosacral screw fixation: early complications of the percutaneous technique. J Orthop Trauma 1997;11(8):584—9.
[11] Routt ML, Simonian PT. Closed reduction and percutaneous skeletal fixation of sacral fractures. Clin Orthop Relat Res 1996;329:121—8.
[12] Tornetta III P, Dickson K, Matta JM. Outcome of rotationally unstable pelvic ring injuries treated operatively. Clin Orthop Relat Res 1996;329:147—51.
[13] Moed BP, Karges DE. Techniques for reduction and fixation of pelvic ring disruptions through the posterior approach. Clin Orthop Relat Res 1996;329:102—14.
[14] van Zwienen CM, van den Bosch EW, Snijders CJ, Kleinrensink GJ, van Vugt AB. Biomechanical comparison of sacroiliac screw techniques for unstable pelvic ring fractures. J Orthop Trauma 2004;18(9):589—95.
[15] Humphrey CA, Liu Q, Templemen DC, Ellis TJ. Locked plates reduce displacement of vertically unstable pelvic fractures in a mechanical testing model. J Trauma 2010;69(5):1230—4.
[16] Kyong SM, Zamorano DP, Wahba GM, Garcia I, Bhata N, Lee TQ. Comparison of two-transsacral-screw fixation versus triangular osteosynthesis for transforaminal sacral fractures. Orthopedics 2014;37(9):754—60.
[17] Pohlemann T, Angst M, Schneider E, Ganz R, Tscherne H. Fixation of transforaminal sacrum fractures: a biomechanical study. J Orthop Trauma 1993;7(2):107—17.
[18] Pohlemann T, Culemann U, Tscherne H. Comparative biomechanical studies of internal stabilization of trans-foraminal sacrum fractures. Orthopade 1992;21:413—21.
[19] Schildhauer TA, Ledoux WR, Chapman JR, Henley MB, Tencer AF, Routt Jr ML. Triangular osteosynthesis and iliosacral screw fixation for unstable sacral fractures: a cadaveric and biomechanical evaluation under cyclic load. J Orthop Trauma 2003;17(1):22—31.
[20] van Zwienen CM, van den Bosch EW, Hoek van Dijke GA, Snijders CJ, van Vugt AB. Cyclic loading of sacroiliac screws in Tile C pelvic fractures. J Trauma 2005;58(5):1029—34.
[21] Min KS, Zamorano DP, Wahba GM, Garcia I, Bahtia N, Lee TQ. Comparison of two-transsacral-screw fixation versus triangular osteosynthesis for transforaminal sacral fractures. Orthopedics 2014;37(9):e754—60.
[22] Choma TJ, Frevert WF, Carson WL, Waters NP, Pfeiffer FM. Biomechanical analysis of pedicle screws in osteoporotic bone with bioactive cement augmentation using simulated in vivo multicomponent loading. Spine (Phila Pa 1976) 2011;36(6):454—62.
[23] Sagi HC, Ordway NR, DiPasquale T. Biomechanical analysis of fixation for vertically unstable sacroiliac dislocations with iliosacral screws and symphyseal plating. J Orthop Trauma 2004;18(3):138—43.
[24] Simonian PT, Harrington RM, Tencer AF. Internal fixation for the transforaminal sacral fracture. Clin Orthop Relat Res 1996;(323):202—9.
[25] Comstock CP, van der Muelen MC, Goodman SB. Biomechanical comparison of posterior internal fixation techniques for unstable pelvic fractures. J Orthop Trauma 1996;10(8):517—22.
[26] Gorczyca JT, Varga E, Woodside T, Hearn T, Powell J, Tile M. The strength of iliosacral lag screws and transiliac bars in the fixation of vertically unstable pelvic injuries with sacral fractures. Injury 1996;27(8):561—4.
[27] Yinger K, Scalise J, Olson SA, Bay BK, Finkemeier CG. Biomechanical comparison of posterior pelvic ring fixation. J Orthop Trauma 2003;17(7):481—7.
[28] Albert MF, Miller ME, MacNaughjton M, Hutton WC. Posterior pelvic fixation using a transiliac 4.5-mm reconstruction plate:

a clinical and biomechanical study. J Orthop Trauma 1993; 7(3):226—32.
[29] Bodzay T, Flóris I, Varadi K. Comparison of stability in the operative treatment of pelvic injuries in a finite element model. Arch Orthop Trauma Surg 2011;131(10):1427—33.
[30] Böhme J, Shim V, Höch A, Mütze M, Müller C, Josten C. Clinical implementation of finite element models in pelvic ring surgery for prediction of implant behavior: a case report. Clin Biomech (Bristol, Avon) 2012;27(9):872—8.
[31] García JM, Doblaré M, Seral B, Seral F, Palanca D, Gracia L. Three-dimensional finite element analysis of several internal and external pelvis fixations. J Biomech Eng 2000;122(5):516—22.
[32] Heller MO, Bergmann G, Deuretzbacher G, Dürselen L, Pohl M, Claes L, et al. Musculo-skeletal loading conditions during walking and stair climbing. J Biomech 2001;34(7):883—93.
[33] Korovessis PG, Magnissalis EA, Deligianni D. Biomechanical evaluation of conventional internal contemporary spinal fixation techniques used for stabilization of complete sacroiliac joint separation: a 3-dimensonal unilaterally isolated experimental stiffness study. Spine (Phil, Pa 1976) 2006;31(25):941—51.
[34] Leighton RK, Waddell JP, Bray TJ, Chapman MW, Simpson L, Martin RB, et al. Biomechanical testing of new and old fixation devices for vertical shear fractures of the pelvis. J Orthop Trauma 1991;5(3):313—7.
[35] Rieger H, Winckler S, Wetterkamp D, Overbeck J. Clinical and biomechanical aspects of external fixation of the pelvis. Clin Biomech (Bristol, Avon) 1996;11(6):323—7.
[36] Rubash HE, Brown TD, Nelson DD, Mears DC. Comparative mechanical performances of some new devices for fixation of unstable pelvic ring fractures. Med Biol Eng Comp 1983;21(6): 657—63.
[37] Sar C, Kilicoglu O. Pediculoiliac screw fixation in instabilities of the sacroiliac complex: biomechanical study and report of two cases. J Orthop Trauma 2003;17(4):262—70.
[38] Shaw JA, Mino DE, Werner FW, Murray DG. Posterior stabilization of pelvic fractures by use of threaded compression rods—case reports and mechanical testing. Clin Orthop Relat Res 1985;192:240—54.
[39] Simonian PT, Routt Jr ML, Harrington RM, Mayo KA, Tencer AF. Biomechanical simulation of the anteroposterior compression injury of the pelvis. An understanding of instability and fixation. Clin Orthop Relat Res 1994;309:245—56.
[40] Varga E, Hearn T, Powell J, Tile M. Effects of method of internal fixation of symphyseal disruptions on stability of the pelvic ring. Injury 1995;26(2):75—80.
[41] Anderson AE, Peters CL, Tuttle BD, Weiss JA. Subject-specific finite element model of the pelvis: development, validation and sensitivity studies. J Biomech Eng 2005; 127(3):364—73.
[42] MacAvoy MC, McClellan RT, Goodman SB, Chien CR, Allen WA, van der Meulen MC. Stability of open-book pelvic fractures using a new biomechanical model of single-limb stance. J Orthop Trauma 1997;11(8):590—3.
[43] Stocks GW, Gabel GT, Noble PC, Hanson GW, Tullos HS. Anterior and posterior internal fixation of vertical shear fractures of the pelvis. J Orthop Res 1991;9(2):237—45.
[44] Routt Jr ML, Nork SE, Mills WJ. Percutaneous fixation of pelvic ring disruptions. Clin Orthop Relat Res 2000;(375):15—29.
[45] Matta JM, Tornetta P. Techniques and outcome in pelvic fractures — internal fixation of unstable pelvic ring injuries. Clin Orthop Relat Res 1996;329:129—40.
[46] Moed BR, Whiting DR. Locked transsacral screw fixation of bilateral injuries of the posterior pelvic ring: initial clinical series. J Orthop Trauma 2010;24(10):616—21.
[47] Moed BR, Fissel BA, Jasey J. Percutaneous transiliac pelvic fracture fixation: cadaver feasibility study and preliminary clinical results. J Trauma 2007;62(2):357—64.
[48] Simonian PT, Routt Jr ML, Harrington RM, Tencer AF. Internal fixation of the unstable anterior pelvic ring: a biomechanical comparison of standard plating techniques and the retrograde medullary superior pubic ramus screw. J Orthop Trauma 1994; 8(6):476—82.
[49] Van den Bosch EW, Van der Kleyn R, Hogervorst M, Van Vugt AB. Functional outcome of internal fixation for pelvic ring fractures. J Trauma 1999;47(2):365—71.